

High-Speed Antagonistic Shape Memory Actuator for High Ambient Temperatures

Rouven Britz,* Gianluca Rizzello, and Paul Motzki

This work presents the development of an innovative shape memory alloy (SMA) actuator principle, which allows high-speed switching cycles through the decoupling of antagonistically arranged SMA wires. Being optimized for the use at high ambient temperatures up to 65 °C, a possible application area is the active venting of injection molds where it can be used to expel air, which is trapped during the injection mold process. The patented actuator principle is based on a decoupled agonist–antagonist SMA-spring system and allows a high-speed closing movement by a compact and lightweight design. Another innovation compared to conventional antagonistic SMA actuator systems is the integrated fail-safe mechanism, which guarantees a defined closed state in case of power failure. Subsequently, in the motivation the need for active venting valves for injection molding is first described. Second, the novel actuator principle is introduced, and the development of an electronics concept is discussed. Finally, the design process, assembly, and validation of two iterations of the actuator prototype are presented. The final prototype validation measurements showcase high performance by valve strokes of 1 mm within 100 ms at ambient temperature of 65 °C.

already widely used in various commercially available products, for example, in industry,^[1–3] the automotive and aerospace sector,^[4–7] the medical field^[8–10] and consumer electronics,^[11–13] and offer the possibility of constructing lightweight, compact, and energy-efficient actuator systems.^[14–20] The underlying mechanism for the use of SMA wires as actuators is their ability to perform a reversible phase transformation at the crystal lattice level.^[20,21] This phase transformation is macroscopically visible in a change of the length (contraction) of the SMA wire up to 4%.^[22,23] Initially at room temperature, the crystal lattice is in a martensitic phase and can undergo a phase transformation to an austenitic crystal structure by applying energy in the form of heat. The technically simplest way to heat a wire is applying an electric voltage, which generates a current flow through the SMA wire. For the use of this effect in an actuator system, which can generate repeated output motion, the

SMA wire needs to be restored to its initial length using a biasing system (e.g., a linear spring).^[24–27]


Due to their high energy density in the range of 10^7 J m^{-3} , SMA wires excel as actuators in compact systems.^[28] This advantage opens up application areas, which are hardly feasible or even not possible with conventional actuators.^[29] The field of valves certainly contains a lot of possible applications that would profit from a more compact and lightweight design but the limited switching frequency and temperature range of SMA technology are still major obstacles on the way to widely spread commercial products. In some of these areas, the environmental conditions, especially high ambient temperatures, are challenging for SMA technology, because of the thermomechanical dependency. An exemplary application area for the latter is injection molding, which motivates this illustration of the capabilities of SMA wires in combination with a suitable mechanical design. In injection molding machines, various valves with different functions are represented. To take full advantage of the compact design possibilities, a venting valve for injection molds was selected for this cases study. Venting of an injection mold is needed to prevent air from being trapped in the cavity, which will lead to a casting failure. Therefore, the vent needs to be closed in a well-defined time slot to prevent the valve tappet from being back injected and simultaneously allow the air sufficient time to leave the cavity. Back-injection means that liquid plastic gets behind the valve

1. Introduction

In industrial applications, conventional nonelectric actuators such as pneumatics will increasingly be replaced in the near future by more energy-efficient electrically actuated drive systems. State-of-the-art electrical solutions are usually built with different kinds of electric motors or electromagnets. As an electric alternative, shape memory alloys (SMAs) can play an important role in this ongoing electrification process. SMA wires are

R. Britz, G. Rizzello, P. Motzki
Department of Systems Engineering
Department of Materials Science and Engineering
Saarland University
Saarbrücken 66123, Germany
E-mail: rouven.britz@imsl.uni-saarland.de

P. Motzki
Center for Mechatronics and Automation Technology (ZeMA gGmbH)
Saarbrücken 66121, Germany

 The ORCID identification number(s) for the author(s) of this article can be found under <https://doi.org/10.1002/adem.202200205>.

© 2022 The Authors. Advanced Engineering Materials published by Wiley-VCH GmbH. This is an open access article under the terms of the Creative Commons Attribution License, which permits use, distribution and reproduction in any medium, provided the original work is properly cited.

DOI: 10.1002/adem.202200205

tappet and blocks this in movement and makes the ejection of the injection molded part impossible.

In this article, a patented novel actuator principle based on SMA wires is presented. Unlike current SMA systems, this origination approach enables high-speed back and forth switching in an antagonistic configuration of SMA actuators. Additionally, this innovative SMA actuator system can be tuned to perform at high ambient temperatures, which is the most common restriction of state-of-the-art SMA-based drives. To illustrate the principle and capabilities of the actuator system, an example application in the field of injection molding is chosen. As an active venting valve in injection molds, the actuator faces the challenges of compact design, high ambient temperatures, and high-speed activation. The developed antagonistic actuator system is based on two actuators, each consisting of an SMA wire, which works against a mechanical bias spring. These two SMA-wire-spring configurations work against each other in only one direction. Specifically, one of these configurations is able to open and close the valve, the opening due to the activation of the SMA wire, the closing is due to the cooling of the SMA wire and the force of the biased spring. Because of the slow cooling behavior of SMA wires, preventing a back injection cannot be ensured. The timing and accurate triggering of opening and closing the valve is necessary for the chosen application. Therefore, the second SMA-wire-spring system can be activated independently from the first and ensures a high-speed closing at the right moment. This is possible due to the decoupling of the two antagonistic working SMA-wire-spring systems in the closing direction.

The subsequent chapters first illustrate the motivation of using SMA wires as actuators in a venting valve in injection molding. Afterward, the actuator concept is explained at the example of a venting valve. Furthermore, the developed control electronics is presented, including the validation of the electronics. The remaining chapters of the article describe the design process, assembly, and validation of two developed prototypes. Starting with the prototype for the proof-of-concept of the mechanism and ending with the second prototype optimized for high-ambient temperatures. Finally, the results of a trial injection mold process with the developed prototype are presented and a conclusion and outlook are given.

2. Motivation

When looking for alternative actuator technologies with the intention of replacing state-of-the-art drives in applications, SMA technology is oftentimes overlooked because they are known for their limited actuation frequency and feasible temperature range. While this holds true for the shape memory material itself, these drawbacks can be attacked and overcome by smart system design and control strategies.^[18,19] The need for fast switching frequencies as well as functionality in higher ambient temperatures in a wide range of possible applications for SMA-based drives has led to the invention of this novel SMA system design approach. The field of injection molding was chosen to exemplarily showcase the ability to overcome the commonly mentioned drawbacks of SMA technology while still maintaining the advantage of their unreached energy-density and ultra-compact system design and integration.

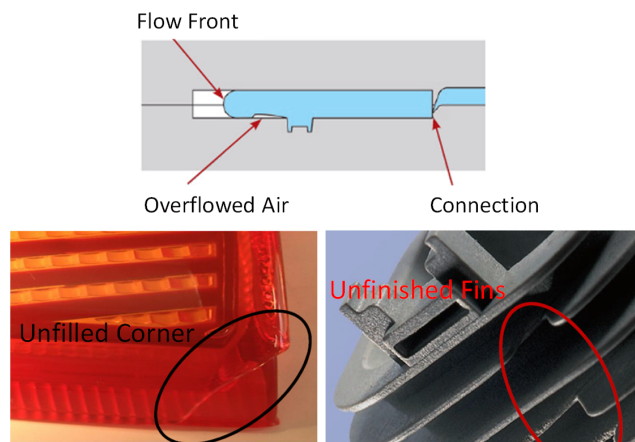


Figure 1. Effects of trapped air in injection molds. Reproduced with permission.^[31] Copyright 2020, ASME.

Injection molding is a widely used technology for mass production of plastic parts. During the injection mold process, when the liquid plastic flows in the cavity, trapped air can prevent a complete filling.^[30] **Figure 1** shows various examples of unfinished injection molded parts because of trapped air. Typically, an injection mold is separated in multiple parts but at least two halves. The state-of-the-art solution to release trapped air in cavities is a passive venting based on small gaps, which are ground between the halves. **Figure 2** explains the passive venting standard solution. Typically, the gaps are designed to generate either no edge or if not possible otherwise, a defined, small edge. Therefore, this method requires high planning effort and precision in production. Furthermore, the separation of the injection mold into at least two halves is essential to place the previously described gaps to release the air.

Additionally, to passive venting, active venting of injection molds represents an alternative approach, where an actuator is used as a valve, which opens a ventilation duct and is closed when the air in the cavity is ejected. **Figure 3a** shows an uncomplete

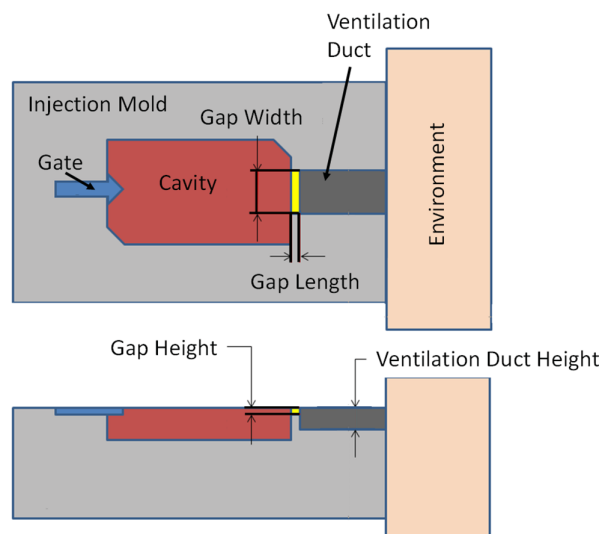


Figure 2. Standard passive venting solution.^[31]

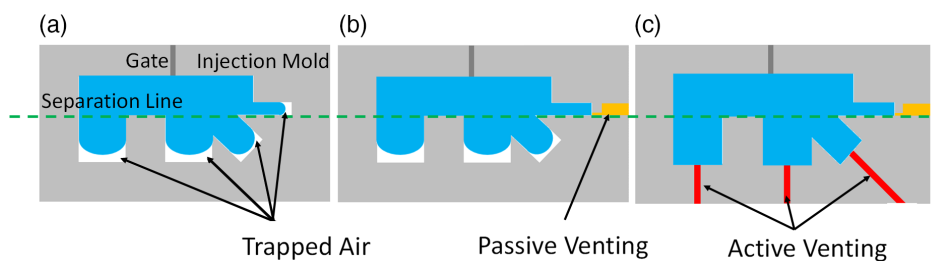


Figure 3. Advantage of an active venting valve.^[31]

filled cavity due to trapped air when not using a venting system. The liquid plastic flows through the gate into the injection mold. While the plastic is shown in blue, the separation line in green indicates the two mold halves which are needed to be able to remove the injection molded part. In Figure 3b, a passive venting gap is positioned at the separation line of the two mold halves. On this position, the air can be expelled and makes a complete fill of the cavity possible if the liquid plastic flows in. Because of the missing separation lines at the other three locations, passive venting gaps cannot be easily implemented. In these cases, a separation of the mold to grind the gaps with a following reassembling would be required. Figure 3c, in contrast, shows the result using active venting valves and illustrates that there is no air left in the mold. By implementing an active venting valve, the advantage is that only drilled holes are needed for the positioning of the valves. This is easily possible at all positions and angles and reduces the effort for the overall venting of the molding process.

The motivation to use an SMA actuator instead of conventional actuators (commonly used electromagnetic systems) is the significantly reduced radial construction space they need (Figure 4). SMA wires can be highly integrated and allow for a compact active venting valve design. This fact leads to an advantage in case of complex injection mold geometries, for example, Figure 1, bottom right. This level of needed vents might be hard, or even impossible, to obtain with conventional, typically electromagnet-driven valves.

3. SMA Actuator Concept

The realized SMA actuator is based on two antagonistically working SMA-wire-spring configurations. As a result of this setup, one SMA-wire-spring-system is depending on the movement of the second system to open the actuator. For an active closing of the actuator, the second SMA-wire-spring-system can operate independently. This special kind of mechanical coupling allows for a fast closing without the need of waiting for the first activated SMA wire to cool down. The mechanical setup also allows for a slow passive closing after deactivating the first SMA wire, which is responsible for opening the valve. In this case, the system response time depends on the cooling rate of the first SMA wire. The advantage is given by a normally closed system, which is necessary to meet the security standards while working with injection molds. This SMA actuator concept is, therefore, different from a standard antagonistic SMA system, in which two wires are working directly against each other.^[32–36]

An example of an injection molding process with a built-in valve is shown in Figure 5, explaining the patented operating principle in a more detailed way.^[37] On the left-hand side, a simplified injection mold cavity with a drilled valve seat is shown. In dark blue and yellow the movable inner parts of the actuator system are shown. They are relatively movable to each other. The grey parts are representing the housing and show the fixed bearings of the springs and SMA wires, which additionally allow

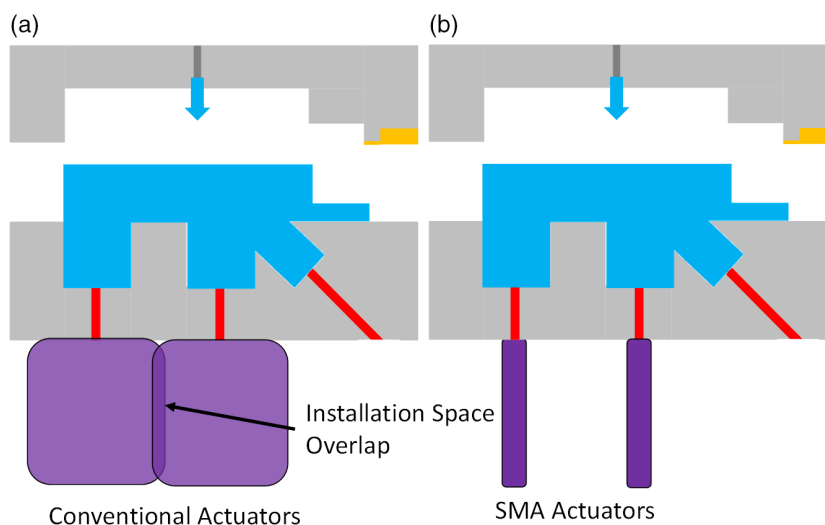


Figure 4. Installation space comparison of conventional and shape memory alloy (SMA) actuators.^[31]

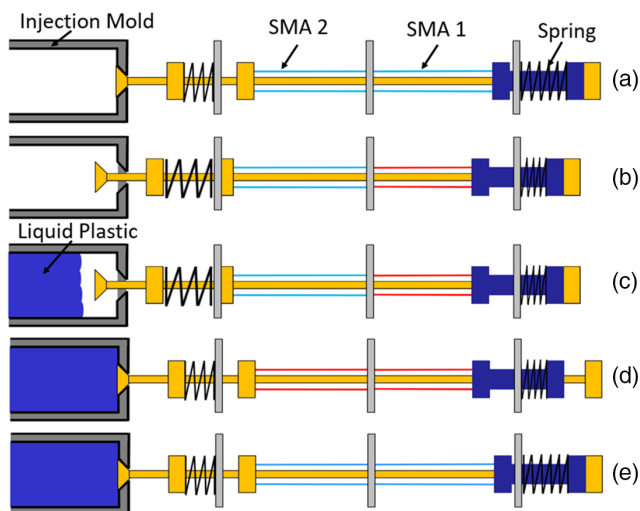


Figure 5. Sketch of the functionality of the actuator using the example of an injection molding process. Reproduced with permission.^[32] Copyright 2020, The Authors, published by Front. Robot. AI.

a guiding of the inner parts. The SMA wires are shown in light blue representing the cold state and red representing the hot state with the compression springs shown in black. Figure 5a shows the initial position of the valve before the injection mold process starts. All SMA wires are in the cold state. The normally closed position as initial position is achieved due to the fact, that the force of the SMA1-spring-system is higher than the force of the SMA2-spring-system. Thus, the spring of the SMA1-spring-system always pushes the valve into the closed position. In Figure 5b, the injection mold process has started, the valve opens by activating SMA 1. Through the activation of SMA 1 and the resulting compression of the spring, the spring of the second SMA-spring-system can relax. If the liquid plastic flows in and displaces the air, the air can escape from the cavity through the open valve. If the plastic reaches the valve (Figure 5c), SMA 2 will be activated and closes the valve immediately (Figure 5d). At the same time, SMA 1 can be deactivated. A closed valve allows the plastic to fill out the cavity completely without a back injection. This is possible through the decoupling of the two SMA systems in the mechanical design, which

facilitates the fast-closing movement independently of the cooling behavior of the opening actuator. The timing to close the valve by activating SMA 2 can be determined by additional sensors or can be time controlled, based on the start of the injection mold process using a flow simulation. As soon as the cavity has been filled completely with plastic, SMA 2 can be deactivated as well, and the valve restores its initial position (Figure 5e). The process can start again after the ejection of the injection molded part.

4. Electronic Concept

The developed electronics allows for an accurate control of the actuator and the communication between the actuator and an injection mold machine. After a trigger signal is detected, the electronics activates the two SMA wires inside the actuator in a specific order to open and close the valve. For the activation, two voltage controlled current sources are used. The current amplitude and activation time of each SMA wire are microcontroller controlled and programmable via universal serial bus (USB). Figure 6 shows the complete circuit board.

Additionally, for future research, the electronic contains two differential amplifiers for measuring the voltage of the SMA wires, thus allowing to exploit the self-sensing effect of SMA wires for condition monitoring or control purposes.^[38–41]

After completing the circuit board, a validation is performed. The whole period of activation is time dependent, started by a trigger signal. First, SMA 1 is activated for a specific time, which is programmable via USB. After SMA 1 turns off, SMA 2 turns on for a specific time, which is also programmable via USB. The activation times and current amplitudes of SMA 1 and SMA 2 are independently programmable. An example of resulting activation periods of the two SMA wires is shown in Figure 7. The black and blue curves indicate the current signal for the two different SMA wires. In the shown period of activation, SMA 1 (valve opening) is activated with a current amplitude of 300 mA for 1 s, while SMA 2 (valve closing) is activated with 400 for 100 ms. This means that the valve is open for 1 s and closes in 100 ms, for which the higher current amplitude of SMA 2 is necessary.

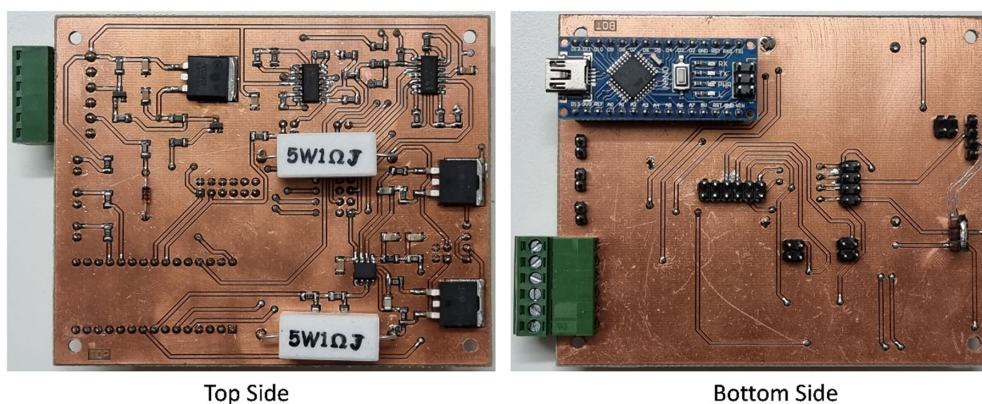


Figure 6. Complete circuit board for activation of the two SMA wires inside the actuator.

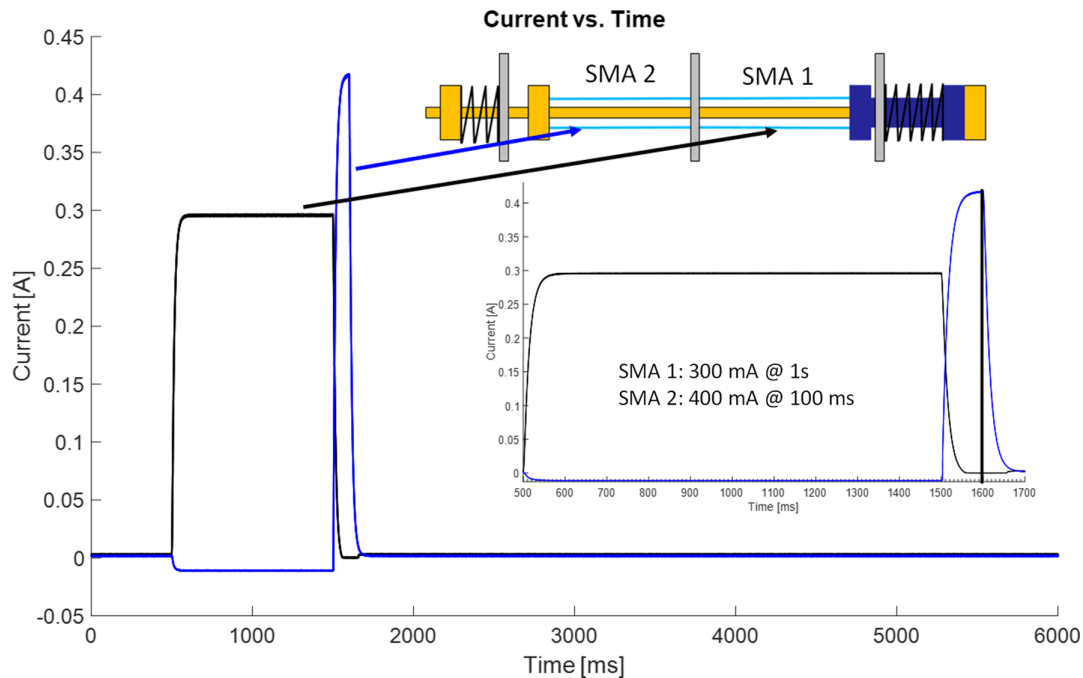


Figure 7. Circuit board validation, example of SMA driving signal.^[31]

5. Proof-of-Concept Mechanism: Design, Assembly and Validation of Prototype I

As a first step, a proof-of-concept prototype is designed and assembled to validate the presented decoupled actuator mechanism in combination with the developed electronics. In addition, the significantly decreased installation space using SMA wires as actuator elements is demonstrated. In this regard, a total maximum outer diameter of 10 mm and a total maximum length of 150 mm are the selected design specifications. For the actuator, a total stroke of $\Delta l = 1$ mm is considered, this allows for a fast venting of the cavity through a proper opening of an air exhaust duct. A means of choice to increase the lifetime of SMA wires is reducing their actuation strain, therefore the actuator design limits the maximum strain to $\varepsilon = 2\%$. With this design parameter, the austenitic (contracted) length l_0 of the SMA wires can be calculated as follows.

$$l_0 = \frac{\Delta l}{\varepsilon} \quad (1)$$

As a result, an austenitic length $l_0 = 50$ mm is calculated. Arranging the SMA wires in a U-shape simplifies the electrical connection as well as enables generating higher forces than using only one wire. Furthermore, the SMA wires have a radial 90° offset and are nested within each other to keep the needed construction space as compact as possible. Figure 8 shows the wire arrangement inside the prototype.

The design considers using commercially available springs as biasing elements with a stiffness of $k = 0.9 \text{ N mm}^{-1}$ and an outer diameter of $D_e = 2.9$ mm. The SMA wire diameter must be adjusted according to the spring. For the calculation, the

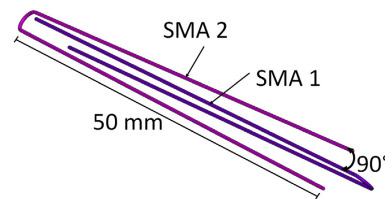


Figure 8. Wire arrangement inside the proof-of-concept prototype.^[31]

maximum force of SMA1-spring-system is essential and set to $F_{\max 1} = 2.7$ N. The U-shape of the SMA wire results in doubling the provided SMA force. Also, to increase the lifetime it is beneficial to reduce the mechanical stress of the wires in actuation. Therefore, a maximum stress $\sigma_{\max 1} = 300$ MPa is chosen. These conditions allow to calculate a wire diameter d as follows.

$$d = \sqrt{\frac{2F}{\pi\sigma}} \quad (2)$$

As a result, an SMA wire diameter of $d = 76 \mu\text{m}$ is chosen.

To facilitate the assembly, the valve design is divided in two halves. In one half, the complete internal structure can be installed and adjusted, the second half functions as a top cover. Figure 9 shows one half-shell with the internal structure and SMA wires. The half-shell (grey) has an outer diameter of 6 mm and an inner diameter of 3.1 mm. The thickest parts of the internal structure have a diameter of 3 mm. To attach the valve mechanism to the actuator, an M2 thread is attached to the tip of the actuator (orange).

The complete actuator design provides for the two half-shells to be pushed into a housing (Figure 10). This keeps the half-

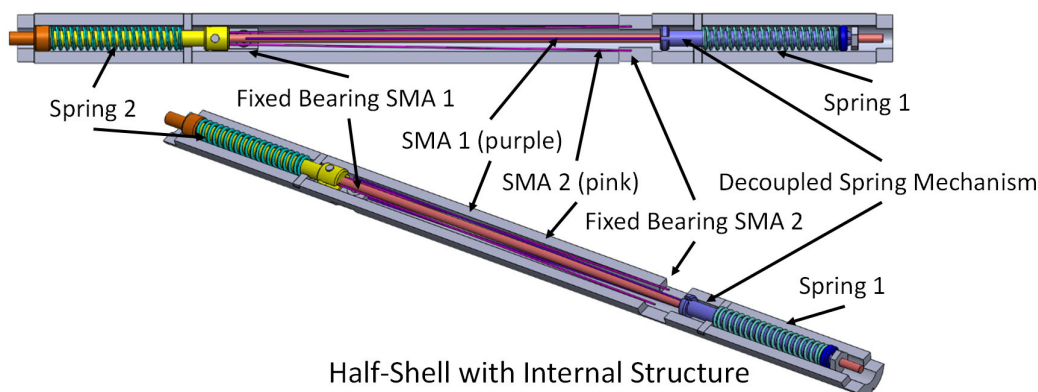


Figure 9. Computer-aided design (CAD) design of the half shell with internal structure.^[31]

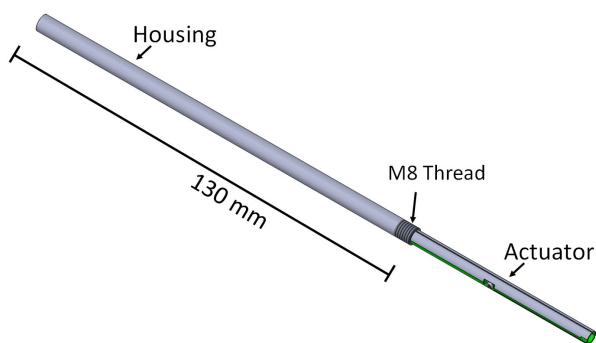


Figure 10. Two half-shells (actuator) pushed together in the housing.^[31]

shells together on the one hand and protecting the inner structure from external influences on the other hand. The housing is 130 mm in total length and has a diameter of 8 mm. The previously mentioned requirements for the dimensions of the actuator are thereby fulfilled. For the electrical connection of the actuator, there is a connector inside the housing. To screw on a plug, the prototype has an M8 thread on the outside of the housing.

After designing the mechanics, the parts are manufactured. The half-shells are manufactured using wire eroding and are made of stainless steel. The inner parts are produced via a lathe and a milling machine and are made of brass. The fixed bearings for the wires and the springs, which are sliding surfaces at the same time, are produced by injection molding, using a high temperature-resistant plastic. To avoid short circuits from the

wires to the other metal parts, the wires are covered in Teflon tubes. For the electrical connection of the SMA wires inside the prototype, enameled copper wires are used. During the assembly, first, the inner parts are positioned in one half-shell. Then the SMA wires are attached to the inner parts and the corresponding fixed bearings. Figure 11 shows the assembly with the inner parts and the SMA wires before the two half-shells are put together.

As a last step during the assembly of the prototype, the half-shells are inserted into the housing (Figure 12, upper part) and the electrical connection is attached. The finished prototype is shown in Figure 12, lower part.

To proof the concept of the decoupled mechanism inside the prototype, an experimental test rig is built, measuring the stroke of the actuator, the current through the SMA wires and the voltage drop over the SMA wires. To simulate the usage in high ambient temperatures as needed in injection molding processes, the test rig allows validating the prototype in a climate chamber. The data is being acquired using an NI cRIO 9074 and LabVIEW. The cRIO is connected to a displacement sensor RC171 from PHILTEC to measure the stroke of the actuator. For the voltage and current measurement, the cRIO is connected to the developed circuit board with integrated measurement points to measure voltage and current of the SMA wires. Additionally, a trigger signal for the developed electronics to activate the actuator is generated from the cRIO. Figure 13 shows the test rig in a block diagram including the actuator inside the climatic chamber.

To validate the actuator performance in combination with the developed electronics, a first experiment is performed. In theory, the actuator should be in the initial position, which is the rear-most position of possible movement. Due to the activation of the

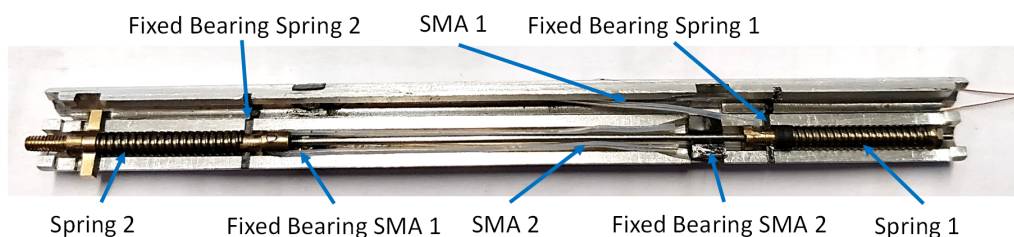


Figure 11. Half-shells with integrated inner parts and SMA wires.^[31]

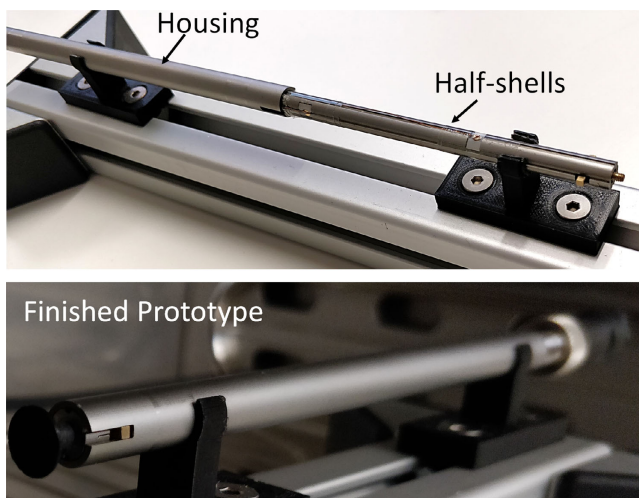


Figure 12. Half-shells inserting into housing (upper part), finished prototype with attached electrical plug (lower part).^[31]

SMA wires, the actuator should do a movement of 1 mm in both directions. In the experiment, SMA 1 is activated for 1 s, which leads to the opening of the valve. After this one second, SMA 1 will be deactivated and SMA 2 will be activated at the same time for 100 ms, leading to the closing of the valve. The results of the experiment are shown in **Figure 14**. The current signals generated from the developed electronics are shown in the upper part of Figure 14. The black signal represents the current through SMA 1. A current amplitude of 300 mA and a duration of 1 s is predefined by programming the electronics and confirmed by the measurement. The blue signal represents the current through SMA 2, the amplitude and duration are also predefined with a value of 400 mA and 100 ms. The mechanical output, as reaction of the activation of the two SMA wires, is shown in the lower part of Figure 14. The current starts flowing through the corresponding wire at 500 and 1500 ms. It can be observed that the stroke response is delayed compared to the current, because of the heating process of the SMA wires. The closing movement is done in 100 ms, starting at 1500 ms. The measurement shows

that the actuator does not reach the required stroke of 1 mm and that the actuator is not at the rearmost position in the initial position. This is indicated by the larger closing movement compared to the opening movement. As a comparison, consider the stroke at 600 and 1500 ms.

A further experiment highlights the decoupled active closing behavior of the actuator in comparison to a passive closing. Active closing describes the closing movement due to the activation of SMA 2, passive closing means the closing movement due to deactivation of SMA 1 and the resulting decompression of spring 1. **Figure 15** displays the results, showing the active closing in black, where a fast decrease of stroke at 1500 ms can be observed. In contrast, the blue curve represents the passive closing, which remains at maximum stroke for a longer period of time and shows a slow decrease of stroke. In both cases, SMA 1 is activated with a 300 mA pulse for 1 s. In addition, the experiment shows that the spring of the closing system is too weak to do a complete passive closing movement.

To validate the actuator performance at a high ambient temperature, the actuator is activated at 65 °C ambient temperature in a climatic chamber. **Figure 16** compares the results of the high-temperature and the low-temperature measurements. At each temperature, the actuator is activated 3 times. It can be seen that the performance at 65 °C is much worse than at 25 °C. The initial starting point is shifted 50 μm toward opening of the valve and the opening movement is only 50 μm. The closing movement is about 250 μm and does not reach the end position. At 1800 ms, a slow cooling behavior of SMA 2 can be seen and the actuator is back in its initial position after ≈3 s of cooling time.

The reason for this poor performance is the transformation temperature of the SMA wires. In high ambient temperature, both wires are partially transformed to austenite, which in summary leads to the different initial point and the weaker performance in movement. To improve the high ambient temperature performance, the transformation temperature can be increased by the pre-stress of the SMA wires. For this reason, a second prototype is built. The next chapter explains the development of a high ambient temperature optimized prototype, which finally will show the same performance at 65 and at 25 °C.

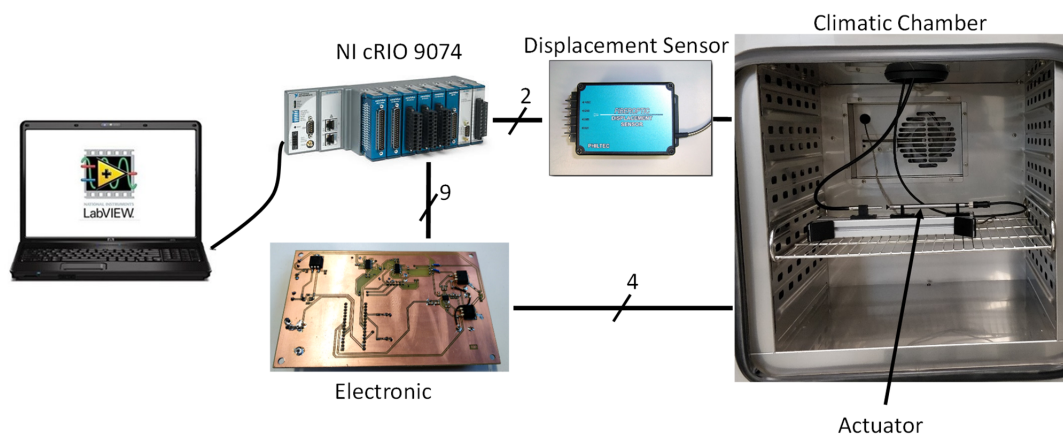


Figure 13. Measurement setup for the validation of the actuator in high ambient temperature environments.^[31]

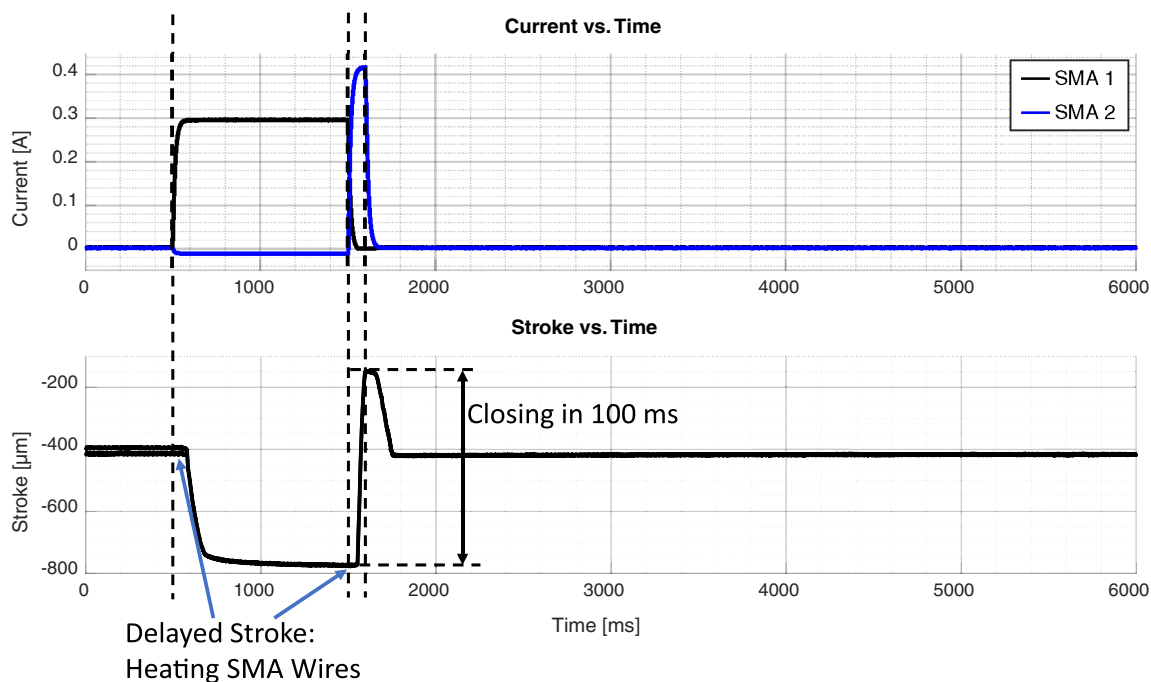


Figure 14. Experiment result of activation SMA 1 for 1 s and SMA 2 for 100 ms.^[31]

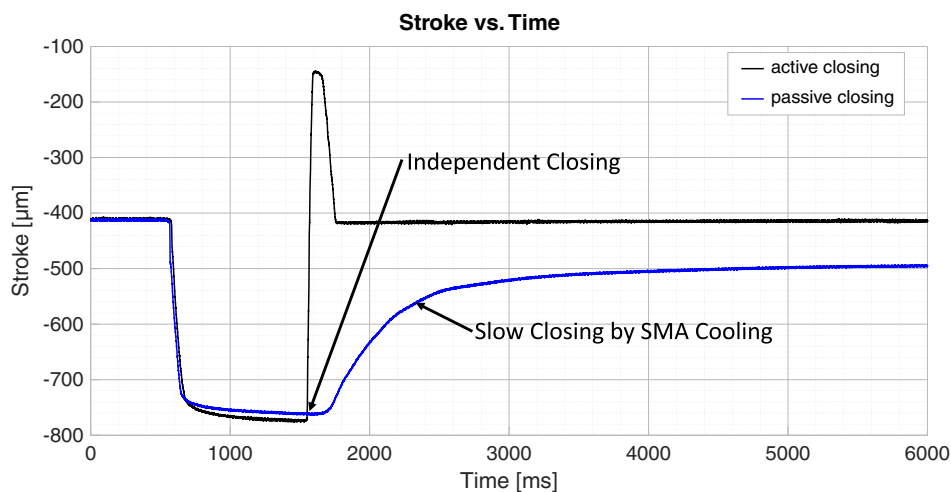


Figure 15. Experimental result of an active closing versus a passive closing movement.^[31]

6. Prototype II: High Ambient Temperature Optimization

The first prototype was able to demonstrate the general functionality of the developed SMA mechanism. In this chapter, the optimization for the use of the actuator in increased ambient temperatures is shown.

The first step in the new design process is the adaption of the two SMA-wire-spring-systems. For this, a simulation tool based on a polycrystalline SMA model^[41] was developed, allowing for predicting the behavior of an SMA-wire-spring-system in high

ambient temperatures. Figure 17 shows the resulting plot of the simulation tool for the SMA-wire-spring-system, which opens the valve. The hysteresis curve of the SMA wire at ambient temperature is shown in blue, in this case 65 °C. Red indicates the SMA hysteresis after heating and the yellow straight shows the characteristic curve of the mechanical bias spring. The result shows the behavior of two wires, mechanically parallel with a diameter of 150 μm and a spring with a stiffness of 6.68 N mm⁻¹ at 65 °C ambient temperature. Two equilibrium points are marking the initial position of the system (blue curve) and the position when the SMA wires are heated (red curve).

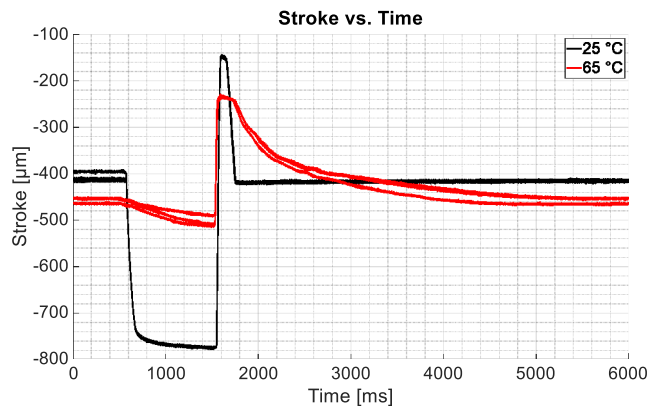


Figure 16. Actuator performance at 25 and 65 °C ambient temperature.^[31]

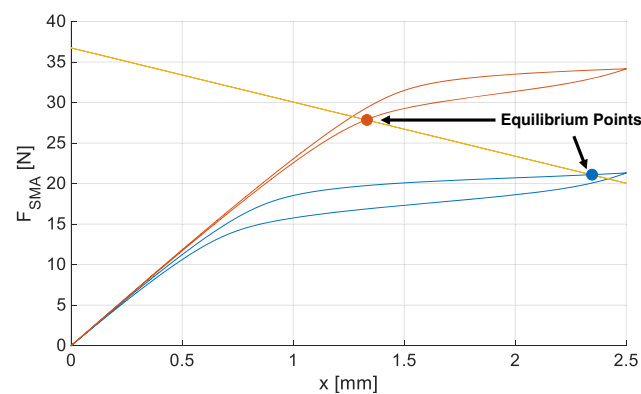


Figure 17. Simulation result for a SMA-spring-system at 65 °C ambient temperature.

The difference of position of both equilibrium points defines the stroke of the actuator system and amounts to 1 mm. The resulting stress for each SMA wire is 597 MPa in the initial state and 788 MPa when heated. To guarantee that the opening SMA-wire-spring-system can do a passive closing, the system is designed to generate approximately double the force in comparison to the closing SMA-wire-spring-system. In the closing SMA-wire-spring-system, SMA wires with a diameter of 100 µm are used. The maximum force of the closing mechanism is 10.3 N, which is equivalent to a stress of 651 MPa per wire.

The final temperature optimized prototype including the electronic box is shown in **Figure 18**. The housing of the prototype is adapted for the usage in an injection molding tool. Before this, a validation of the actuator is done and shown in **Figure 19**. The upper part of **Figure 19** shows the current signals generated from the developed electronics. The current signals of the two wires at an ambient temperature of 25 °C are shown in black, pink describes the current signals of both SMA wires at an ambient temperature of 65 °C. Because of the higher ambient temperature, there is less energy needed to heat the wire to its transformation temperature. Therefore, a lower current is required at higher ambient temperatures, which is consequently shown in the two current signals. The lower part of **Figure 19** shows the resulting stroke due to the activation of the wires at different ambient temperatures. Blue indicates the stroke at 25 °C ambient

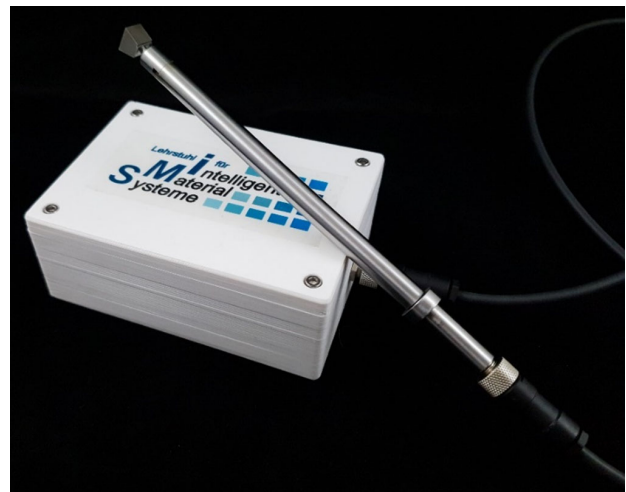


Figure 18. Final temperature optimized prototype with electronic box.

temperature and red shows the stroke at 65 °C. The measurement shows a nearly complete identical behavior at both temperatures. The initial position of the actuator is in the fully closed position and the required maximum stroke of 1 mm can be considered as sufficiently achieved with a generated stroke of more than 950 µm (**Figure 19** at 1500 ms). The fast-closing movement reaches the initial position in 100 ms. After the fast closing, the actuator bounces back in a middle position at 2000 ms. The reason for this is that both SMA wires are deactivated at this time. The resulting middle position is a product of the cooling behavior of the used SMA wires and both springs. One possibility to avoid this bouncing behavior is to keep the SMA 2 activated until SMA 1, which is responsible for opening the valve, has cooled down. After SMA 1 has cooled down, the spring 1 keeps the actuator in the initial position and SMA 2 can cool down as well. However, the systematically conditioned side-effect of the middle position shows that passive closing is ensured by spring 1. Also, it is shown that the passive closing takes more time at higher ambient temperatures because of the slower cooling behavior of the SMA wires. The measurement shows some ripples in the movement, which indicates friction in the prototype.

After the validation with the conclusion that the final prototype functions are given as desired, the prototype is subjected to a field test and is built into an injection molding tool. **Figure 20** shows the prototype in the injection molding tool. In advance, flow simulation is used to determine the point at which air entrapment would occur in the cavity, and the prototype is positioned at this position. The shown injection molding tool including the prototype is used to perform trial injection molds. A trial injection mold with an inactive prototype is performed to validate the flow simulation and to make sure that the prototype is located in the right position in the cavity. On the left in **Figure 21**, the result of the trial injection mold with inactive prototype is shown. Predicted correctly, a casting failure due to the trapped air is the result. In a next step, a trial injection mold with the active prototype is conducted. The result is shown on the right-hand side of **Figure 21**. Since the air can escape, the trial results in a successful cast without any trapped air.

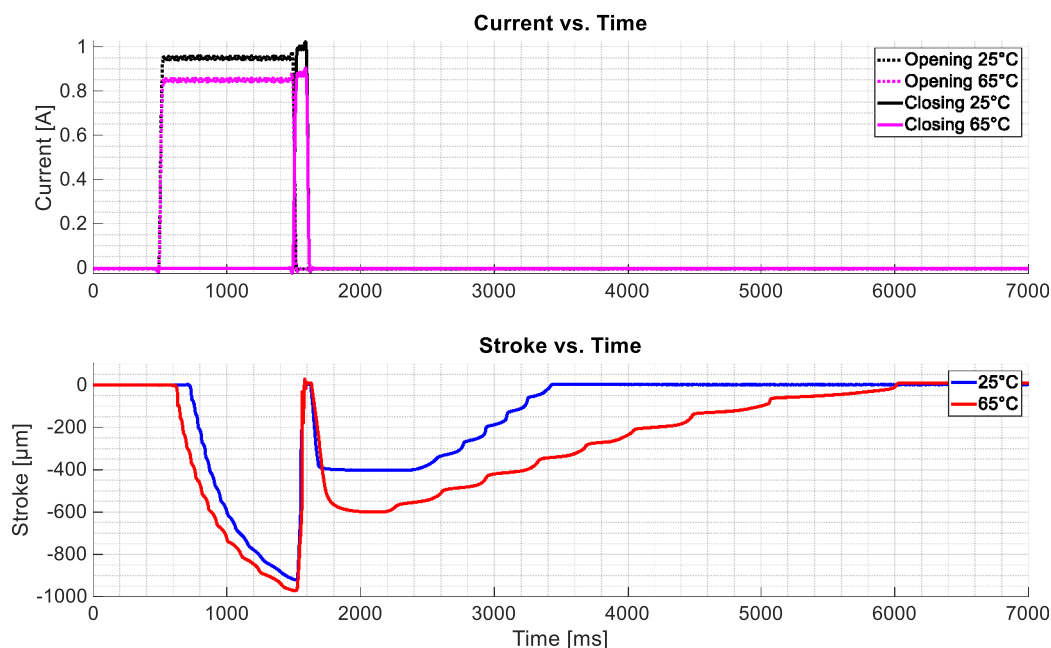


Figure 19. Validation result of the final prototype at different ambient temperatures.

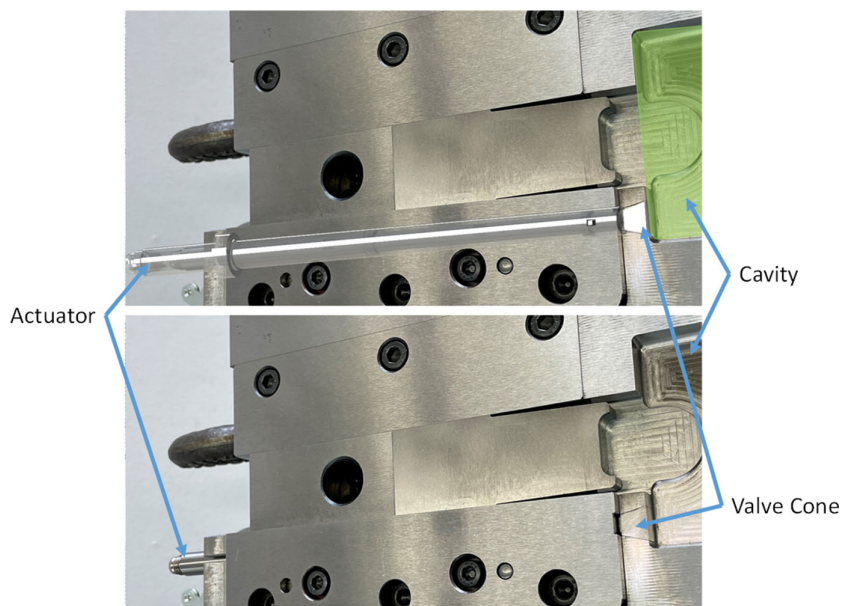


Figure 20. Final prototype built in an injection molding tool.

7. Conclusion and Outlook

This article has presented the development and the validation results of a novel decoupled antagonistic SMA actuator. The actuator is optimized for the usage in high ambient temperature, which is validated via test rig and experimentally confirmed by the trial inserts as an active injection mold venting valve. The motivation for the necessity of venting injection molds has been described. Then, the operating principle of the decoupled antagonistic SMA actuator is presented. To guarantee

the correct activation of the SMA wires, an electronics concept is developed. This ensures the opening and fast closing of the valve at defined times in an injection mold process. The circuit board consists of two programmable current sources, which allow to predefine the current amplitude and activation time of each SMA wire. The first developed prototype serves as the proof-of-concept for the novel actuator concept. The design and assembly process for the first prototype is described as well as the assembled test rig. Experiments at different ambient temperatures show that the actuator concept works correctly, with the

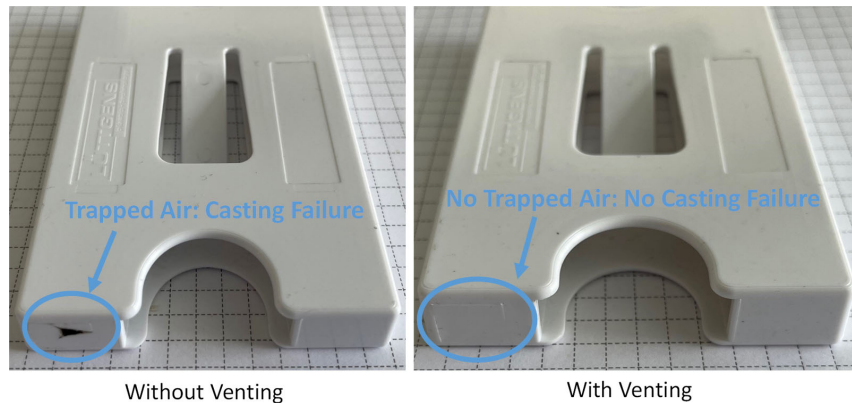


Figure 21. Results of the injection molding process—without activation of the prototype (left), with activation of the prototype (right).

restriction of a decrease in performance at elevated ambient temperatures. For this reason, a second prototype is built with an optimized design. For the design, a simulation tool that allows the prediction of the SMA-system behavior at high ambient temperatures is used. The validation results of the final prototype are shown with the conclusion that the actuator works independently of the ambient temperature. In a final experiment, a test injection mold including the developed actuator as a venting valve is conducted. This field test confirms the test rig experiments and shows the potential of active venting valves avoiding miscasts due to trapped air.

In future steps, the long-life ability of the actuator will be under investigation. These life-cycle tests are carried out in a test rig as well as in an injection molding process. Also, an improvement of the gliding surfaces inside the final prototype will be necessary to avoid the shown ripples in the movement which suggest friction in the bearings.

Acknowledgements

Funded by the Federal Ministry of Education and Research (BMBF) as part of the “KMU-NetC” Program. In addition, the authors would like to thank our project partners Dietrich Lüttgens GmbH & Co.KG and Kunststoff-Institut für die mittelständische Wirtschaft NRW GmbH (K.I.M.W.) for the consistently good cooperation, the production of components, the experiments carried out and the provision of images.

Open Access funding enabled and organized by Projekt DEAL.

Conflict of Interest

The authors declare no conflict of interest.

Data Availability Statement

The data that support the findings of this study are available from the corresponding author upon reasonable request.

Keywords

antagonistic actuator system, high temperature, injection molding, miniaturized actuator system, shape memory alloys, valve

Received: February 10, 2022

Published online: May 3, 2022

- [1] M. Sreekumar, T. Nagarajan, M. Singaperumal, M. Zoppi, R. Molfino, *Ind. Rob.* **2007**, 34 285.
- [2] P. Motzki, S. Seelecke, *Reference Module in Materials Science and Materials Engineering*, Elsevier Amsterdam, **2019**.
- [3] W. Wang, S.-H. Ahn, *Soft Robot.* **2017**, 4 379.
- [4] D. Stoeckel, *Shape Memory Actuators for Automotive Applications*, Materials & Design, **1990**, 11, No. 6.
- [5] Actuator Solutions GmbH and A. S. GmbH, *Actuator Solutions SMA Products*, the company Actuator solutions GmbH, Gunzenhausen, **2018**.
- [6] R. Pecora, I. Dimino, *Shape Memory Alloy Engineering: For Aerospace, Structural and Biomedical Applications*, Butterworth-Heinemann, Oxford, **2014**.
- [7] D. J. Hartl, D. C. Lagoudas, *Proc. Inst. Mech. Eng., Part G* **2007**, 221, 535.
- [8] C. S. Loh, H. Yokoi, T. Arai, in *2005 IEEE Engineering in Medicine and Biology 27th Annual Conf.*, **2005**, pp. 6900–6903, <https://doi.org/10.1109/IEMBS.2005.1616092>.
- [9] M. Leester-Schädel, B. Hoxhold, C. Lesche, S. Demming, S. Büttgenbach, *Microsyst. Technol.* **2008**, 14, 697.
- [10] A. T. Tung, B. H. Park, G. Niemeyer, D. H. Liang, *IEEE/ASME Trans. Mechatron.* **2007**, 12, 439.
- [11] J. B. Gault, S. D. Bowers, J. S. Campbell, A. E. Hillyerd, Y. Aldeharryat, K. Aagaard, E. P. Witt, *Locking Mechanism*, **2019**.
- [12] Cambridge Mechatronics Ltd., CML OIS actuator, [Online], <https://www.cambridgemechatronics.com/en/cml-technology/actuators/> (accessed: April 2020.)
- [13] D. Clausi, H. Gradin, S. Braun, J. Peirs, D. Reynaerts, G. Stemme, W. van der Wijngaart, in *2011 IEEE 24th Inter. Conf. on Micro Electro Mechanical Systems*, January **2011**, pp. 1281–1284, <https://doi.org/10.1109/MEMSYS.2011.5734667>.
- [14] R. Velázquez, E. Pissaloux, J. Szewczyk, M. Hafez, in *Proc. - IEEE Inter. Conf. on Robotics and Automation*, Vol. 2005, **2005**, pp. 1344–1349, <https://doi.org/10.1109/ROBOT.2005.1570302>.
- [15] D. Reynaerts, H. Van Brussel, *Mechatronics* **1998**, 8, 635.
- [16] C. C. Lan, J. H. Wang, C. H. Fan, *Sens. Actuators, A* **2009**, 153, 258.
- [17] J. Mohd Jani, M. Leary, A. Subic, M. A. Gibson, *Mater. Des.* **2014**, 56, 1078.
- [18] P. Motzki, *Efficient SMA Actuation — Design and Control Concepts*, VDI-Expertenforum: Smart Materials, Renningen, **2020**, <https://doi.org/10.3390/IeCAT2020-08520>.

- [19] P. Motzki, T. Gorges, M. Kappel, M. Schmidt, G. Rizzello, S. Seelecke, *Smart Mater. Struct.* **2018**, *27*, 075047.
- [20] D. C. Lagoudas, *Shape Memory Alloys: Modeling and Engineering Applications*, Springer, New York **2008**.
- [21] H. Funakubo, *Shape Memory Alloys*, vol. 1, no. D., Gordon and Breach Science Publ., Amsterdam, **1987**.
- [22] Dynalloy, *Technical Characteristics of Actuator Wires*, Dynalloy Inc, pp. 1–12.
- [23] S. A. E. S. Getters, *SmartFlex Brochure*, Italy, **2017**.
- [24] S. Langbein, A. Czechowicz, *Konstruktionspraxis Formgedächtnistechnik*, Vol. 1, Springer Fachmedien, Wiesbaden **2013**.
- [25] P. Motzki, F. Khelifa, L. Zimmer, M. Schmidt, S. Seelecke, *IEEE/ASME Trans. Mechatron.* **2019**, *24*, 293.
- [26] J. Luntz, B. Barnes, D. Brei, P. W. Alexander, A. Browne, N. L. Johnson, in *Proc. Volume 7290, Industrial and Commercial Applications of Smart Structures Technologies 2009*, SMA wire actuator modular design framework, **2009**, <https://doi.org/10.1117/12.816752>.
- [27] S. Jung, J. Bae, I. Moon, in *Control. Autom. Syst. (ICCAS), 2011 11th Int. Conf.*, **2011**.
- [28] H. Janocha, *Unkonventionelle Aktoren - Eine Einführung*, Oldenburg Verlag, München **2010**.
- [29] S. Akbari, A. H. Sakhaei, S. Panjwani, K. Kowsari, A. Serjoureji, Q. Ge, *Sens. Actuators, A* **2019**, *290*, 177.
- [30] D. O. Kazmer, *Injection Mold Design Engineering*, 2nd ed., München, Carl Hanser Verlag GmbH Co KG **2016**.
- [31] R. Britz, S. Seelecke, G. Rizzello, P. Motzki, in *ASME 2020 Conf. on Smart Materials, Adaptive Structures and Intelligent Systems, SMASIS 2020*, **2020**, pp. 1–6, [https://urldefense.com/v3/___https://doi.org/10.1115/SMASIS2020-2214___!!N11eV2iwtfs!q6l0zt0g1ElQpQqwLfa3HMDce-KAlQrEUrO-S8OAAobqNshr_vz1lwr3qMRF_AoRS7NgOvsE1Eb8_NKCI578LODIMbDI8TqOiQ\\$](https://urldefense.com/v3/___https://doi.org/10.1115/SMASIS2020-2214___!!N11eV2iwtfs!q6l0zt0g1ElQpQqwLfa3HMDce-KAlQrEUrO-S8OAAobqNshr_vz1lwr3qMRF_AoRS7NgOvsE1Eb8_NKCI578LODIMbDI8TqOiQ$).
- [32] F. Simone, G. Rizzello, S. Seelecke, P. Motzki, *Front. Robot. AI* **2020**, *7*, <https://doi.org/10.3389/frobt.2020.608841>.
- [33] R. Featherstone, Y. H. Teh, *Springer Tracts Adv. Robot.* **2006**, *67* https://doi.org/10.1007/11552246_7.
- [34] J. H. Mabe, F. T. Calkins, M. B. Alkisar, in *Proc. Volume 6930, Industrial and Commercial Applications of Smart Structures Technologies 2008*, Variable area jet nozzle using shape memory alloy actuators in an antagonistic design, **2008**, <https://doi.org/10.1117/12.776816>.
- [35] A. Ianagui, E. A. Tannuri, *Mechatronics* **2015**, *30*, 126.
- [36] M. Kohl, B. Krevet, E. Just, *Sens. Actuators, A* **2002**, *97–98*, 646.
- [37] R. Britz, P. Motzki, S. Seelecke, *Thermal Actuator Arrangement Having Improved Reset Time*, **2019**.
- [38] C. C. Lan, C. M. Lin, C. H. Fan, *IEEE/ASME Trans. Mechatronics* **2011**, *16*, 141.
- [39] S. K. Chaitanya, K. Dhanalakshmi, *Demonstration of Self-Sensing in Shape Memory Alloy Actuated Gripper*, in *IEEE International Symposium on Intelligent Control-Proceedings*, **2013**, <https://doi.org/10.1109/ISIC.2013.6658620>.
- [40] T. R. Lambert, A. Gurley, D. Beale, *Smart Mater. Struct.* **2017**, *26* 35004.
- [41] G. Rizzello, M. A. Mandolino, M. Schmidt, D. Naso, S. Seelecke, *Smart Mater. Struct.* **2019**, *28*, 025020.